Science
AAAS

A Crystal Structure of the Bifunctional Antibiotic Simocyclinone D8, Bound to DNA Gyrase

Marcus J. Edwards, *et al.*

Science **326**, 1415 (2009);
DOI: 10.1126/science.1179123

the canonical TnaC sequence, indicating that even residues unrelated to the stalling process can adopt a distinct conformation within the exit tunnel. This notion is supported by a cryo-EM structure of a yeast 80*S* ribosome-nascent chain complex stalled during the translation of a truncated dipeptidyl-aminopeptidase B (DP120) mRNA at 6.1 Å resolution (*27*). Although the DP120 sequence has no stalling capacity, density for this nascent chain is visible, indicating a preferred conformation within the exit tunnel (Fig. 4D). Notably, the DP120 nascent chain follows a different path from that reported here for TnaC (Fig. 4, E and F). Clearly the chemical and electrostatic properties of the tunnel environment play a pivotal role in facilitating this kind of distinct nascent chain behavior (*3*, *4*). The finding that nascent chains with little or no sequence conservation interact with the exit tunnel in a distinct manner and adopt individual conformations may be important not only for initial folding events (*1*–*3*) but also for the variety of nascent chain–mediated regulatory mechanisms (*5*).

References and Notes

1. C. A. Woolhead, P. J. McCormick, A. E. Johnson, *Cell* **116**, 725 (2004).
2. J. Lu, C. Deutsch, *Biochemistry* **44**, 8230 (2005).
3. J. Lu, C. Deutsch, *Nat. Struct. Mol. Biol.* **12**, 1123 (2005).
4. J. Lu, C. Deutsch, *J. Mol. Biol.* **384**, 73 (2008).
5. T. Tenson, M. Ehrenberg, *Cell* **108**, 591 (2002).
6. H. Nakatogawa, K. Ito, *Cell* **108**, 629 (2002).
7. C. A. Woolhead, A. E. Johnson, H. D. Bernstein, *Mol. Cell* **22**, 587 (2006).
8. M. N. Yap, H. D. Bernstein, *Mol. Cell* **34**, 201 (2009).
9. D. Oliver, J. Norman, S. Sarker, *J. Bacteriol.* **180**, 5240 (1998).
10. F. Gong, C. Yanofsky, *Science* **297**, 1864 (2002).
11. L. Cruz-Vera, S. Rajagopal, C. Squires, C. Yanofsky, *Mol. Cell* **19**, 333 (2005).
12. L. R. Cruz-Vera, C. Yanofsky, *J. Bacteriol.* **190**, 4791 (2008).
13. F. Gong, K. Ito, Y. Nakamura, C. Yanofsky, *Proc. Natl. Acad. Sci. U.S.A.* **98**, 8997 (2001).
14. Materials and methods are available as supporting material on *Science* Online.
15. L. G. Trabuco, E. Villa, K. Mitra, J. Frank, K. Schulten, *Structure* **16**, 673 (2008).
16. P. I. de Bakker, N. Furnham, T. L. Blundell, M. A. DePristo, *Curr. Opin. Struct. Biol.* **16**, 160 (2006).
17. M. Simonovic, T. A. Steitz, *Biochim. Biophys. Acta* **1789**, 612 (2009).
18. R. Yang, L. R. Cruz-Vera, C. Yanofsky, *J. Bacteriol.* **191**, 3445 (2009).
19. N. Vazquez-Laslop, C. Thum, A. S. Mankin, *Mol. Cell* **30**, 190 (2008).
20. L. R. Cruz-Vera, A. New, C. Squires, C. Yanofsky, *J. Bacteriol.* **189**, 3140 (2007).
21. T. M. Schmeing, K. S. Huang, S. A. Strobel, T. A. Steitz, *Nature* **438**, 520 (2005).
22. T. M. Schmeing, K. S. Huang, D. E. Kitchen, S. A. Strobel, T. A. Steitz, *Mol. Cell* **20**, 437 (2005).
23. L. R. Cruz-Vera, M. Gong, C. Yanofsky, *Proc. Natl. Acad. Sci. U.S.A.* **103**, 3598 (2006).
24. A. Weixlbaumer *et al.*, *Science* **322**, 953 (2008).
25. K. Mitra *et al.*, *Mol. Cell* **22**, 533 (2006).
26. P. Nissen, J. Hansen, N. Ban, P. B. Moore, T. A. Steitz, *Science* **289**, 920 (2000).
27. T. Becker *et al.*, *Science* **326**, 1369 (2009). Published online 29 October 2009; 10.1126/science.1178535.

28. This research was supported by grants from the Deutsche Forschungsgemeinschaft SFB594 and SFB646 (to R.B.), SFB740 (to T.M.), and WI3285/1-1 (to D.N.W.); by NIH grants GM022778 (to T.A.S.) and P41-RR05969 (to K.S.); by NSF grant PHY0822613 (to K.S.); and by the European Union and Senatsverwaltung für Wissenschaft, Forschung und Kultur Berlin (UltraStructureNetwork, Anwenderzentrum). Computer time for MDFF was provided through an NSF Large Resources Allocation Committee grant MCA93S028. Coordinates of the atomic models of TnaC-70*S* complex have been deposited in the PDB under accession numbers 2WWL (30*S*) and 2WWQ (50*S*). The cryo-EM map has been deposited in the 3D-EM database under accession number EMD-1657.

Supporting Online Material

www.sciencemag.org/cgi/content/full/1177662/DC1
Materials and Methods
Figs. S1 to S9
Table S1
Movie S1
References

12 June 2009; accepted 21 October 2009
Published online 29 October 2009;
10.1126/science.1177662
Include this information when citing this paper.

A Crystal Structure of the Bifunctional Antibiotic Simocyclinone D8, Bound to DNA Gyrase

Marcus J. Edwards,[1] Ruth H. Flatman,[1] Lesley A. Mitchenall,[1] Clare E.M. Stevenson,[1] Tung B.K. Le,[2] Thomas A. Clarke,[3] Adam R. McKay,[4] Hans-Peter Fiedler,[5] Mark J. Buttner,[2] David M. Lawson,[1] Anthony Maxwell[1]*

Simocyclinones are bifunctional antibiotics that inhibit bacterial DNA gyrase by preventing DNA binding to the enzyme. We report the crystal structure of the complex formed between the N-terminal domain of the *Escherichia coli* gyrase A subunit and simocyclinone D8, revealing two binding pockets that separately accommodate the aminocoumarin and polyketide moieties of the antibiotic. These are close to, but distinct from, the quinolone-binding site, consistent with our observations that several mutations in this region confer resistance to both agents. Biochemical studies show that the individual moieties of simocyclinone D8 are comparatively weak inhibitors of gyrase relative to the parent compound, but their combination generates a more potent inhibitor. Our results should facilitate the design of drug molecules that target these unexploited binding pockets.

Bacterial diseases remain a major problem because of the emergence of drug-resistant bacteria combined with the dearth of new antibacterial agents. Despite extensive efforts, there remain relatively few effective drug targets for antibacterials. One of these is the enzyme DNA gyrase, a DNA topoisomerase that controls the topology of DNA (*1*, *2*). Topoisomerases are classified into two types, I and II, depending on whether they catalyze reactions involving the transient breakage of one or both strands of DNA. Gyrase is the only type II DNA topoisomerase that can catalyze DNA supercoiling; this reaction is driven by the free energy of adenosine triphosphate (ATP) hydrolysis (*3*). Gyrase consists of two subunits, GyrA and GyrB (97 kD and 90 kD, respectively, in *Escherichia coli*), which form an A_2B_2 complex in the active enzyme. Because gyrase is essential in bacteria and lacking in humans, it is a valuable drug target (*4*). The complexity of the gyrase supercoiling reaction presents multiple opportunities for intervention. Two well-known groups of gyrase-specific antibacterial agents are quinolones and aminocoumarins. Fluoroquinolones, such as ciprofloxacin, are highly successful drugs (*5*), but their usefulness is diminishing as a consequence of bacterial resistance (*6*). Aminocoumarins, e.g., novobiocin and clorobiocin, are less successful clinically because of toxicity and solubility issues but are very well characterized in terms of their mode of action on gyrase (*7*), including several crystal structures (*8*–*11*). Aminocoumarins act by competitively inhibiting the binding of ATP to the GyrB subunit (*11*). The cloning and sequencing of the biosynthetic pathways for the aminocoumarins novobiocin, clorobiocin, and coumermycin A_1 and the application of bioengineering methodologies (*12*) have enabled the production of a series of modified aminocoumarins with varying potencies against their targets, gyrase and topoisomerase IV (*13*, *14*). This work has raised the possibility of engineering antibacterial agents targeted to gyrase that are based on natural antibiotics.

Simocyclinone D8 (SD8) was isolated from *Streptomyces antibioticus* Tü 6040 (*15*–*18*). The antibiotic consists of a chlorinated aminocoumarin (AC) linked to an angucyclic polyketide (PK) via

[1]Department of Biological Chemistry, John Innes Centre, Colney, Norwich NR4 7UH, UK. [2]Department of Molecular Microbiology, John Innes Centre, Colney, Norwich NR4 7UH, UK. [3]School of Biological Sciences, University of East Anglia, Norwich NR4 7TJ, UK. [4]Department of Chemistry, University College London, 20 Gordon St, London WC1H 0AJ, UK. [5]Mikrobiologisches Institut, Eberhard-Karls-Universität Tübingen, Auf der Morgenstelle 28, D-72076 Tübingen, Germany.

*To whom correspondence should be addressed. E-mail: tony.maxwell@bbsrc.ac.uk

a tetraene linker and a D-olivose sugar (Fig. 1). Because of the presence of the AC moiety, the expectation was that SD8 would target the adenosine triphosphatase (ATPase) domain of GyrB. Although SD8 is a potent inhibitor of *E. coli* gyrase, it does not inhibit the intrinsic GyrB ATPase activity. Instead, SD8 binds to the N-terminal domain of GyrA and prevents DNA binding (*19*). In hindsight, this is not surprising because SD8 lacks the decorated noviose sugar that is attached to the 7-OH of the AC ring and is involved in the majority of the interactions with GyrB in other aminocoumarins (*8*–*11*). In contrast to quinolones and aminocoumarins, which can act on both gyrase and its close relative topoisomerase IV, SD8 is potent against gyrases from *E. coli* and *Staphylococcus aureus* but much less effective against topoisomerase IV from these species (*20*).

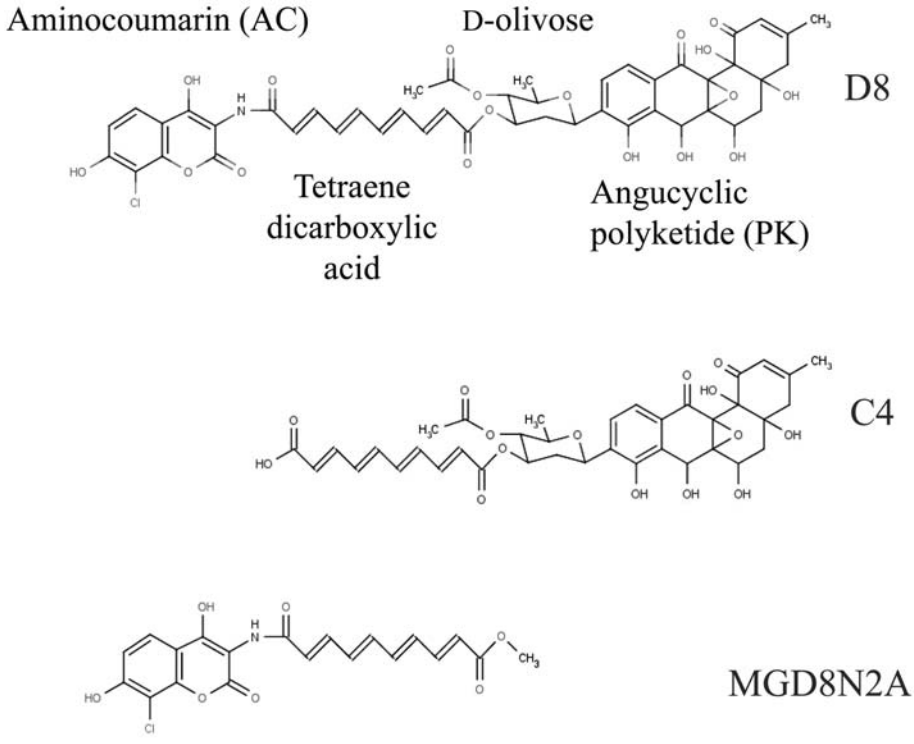

Fig. 1. Structure of simocyclinone D8 and analogs. IC_{50} values for inhibition of supercoiling by gyrase: for D8, 0.6 μM; C4, 70 μM; MGD8N2A, 50 μM.

We have crystallized the N-terminal domain of GyrA (GyrA59) complexed with SD8 and determined the crystal structure at 2.6-Å resolution by molecular replacement from the structure of unliganded GyrA59 that was previously determined (*21*). Our structure reveals a ligand-stabilized homotetramer of GyrA59 subunits consisting of two A59 dimers cross-linked by four molecules of SD8 (Fig. 2). The tetraene linker of SD8 acts as an extended rod, about 10 Å long, that holds the AC and PK moieties apart. Each GyrA subunit has distinct pockets that accept the AC and PK groups, respectively, of two separate SD8 molecules; both pockets lie in the predicted DNA binding saddle. Additional lobes of electron density adjacent to the PK moiety have been modeled as Mg^{2+} ions (Fig. 3A and fig. S1). Although each subunit interacts with two SD8 molecules, because each of these molecules is shared by two subunits from opposing dimers, the stoichiometry remains 1:1, consistent with previous experiments (*19*). In addition to the SD8-mediated dimer-dimer interactions, there is about 1500 $Å^2$ of protein-protein interface. This includes 12 hydrogen bonds, 10 of which involve residues spanning Leu^{17} to Asp^{23}, a region just before α-helix 1 that was not visible in the original GyrA59 structure (*21*). Superposition of the SD8 complex and ligand-free GyrA59 structures gives root mean square deviation values below 1 Å, both for

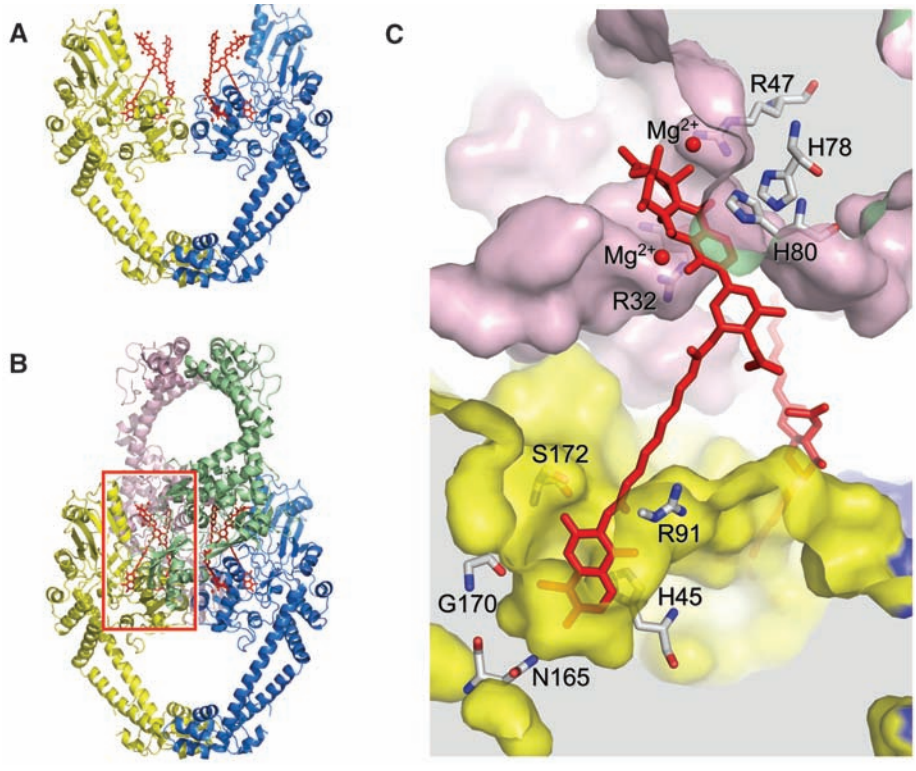

Fig. 2. Crystal structure of the GyrA59-simocyclinone complex. The protein is depicted in cartoon representation, the SD8 molecules are shown as red sticks, and their associated Mg^{2+} ions as small spheres. (**A**) Structure of the GyrA59 dimer and the four SD8 molecules it interacts with. (**B**) Structure of the SD8-mediated tetramer (dimer of dimers). (**C**) Close-up of the red boxed region in (B) showing a section through the complex containing two SD8 molecules. The same color scheme is adopted as for (A) and (B), but the GyrA59 subunits are represented as semi-transparent molecular surfaces. Regions with a white background are either outside the complex or between the subunits; regions with a gray background are within the molecular envelopes. Key residues (*23*) that are close to the SD8 molecule in the foreground are displayed in stick representation.

subunit-subunit and dimer-dimer comparisons, indicating that there are no major conformational changes upon ligand binding (fig. S2). Intriguingly, a single SD8 molecule can be modeled in a "bent" conformation such that it bridges between the AC and PK pockets of the same subunit, while maintaining essentially the same contacts with the protein seen in the crystal structure (fig. S3). This places the tetraene linker close to, and possibly interacting with, α-helix 4.

To investigate the oligomeric state in solution, we performed a series of molecular weight (MW) studies. Analytical ultracentrifugation (table S2) showed that the MW of GyrA59 in the absence of SD8 or at low ligand:protein ratios (<~3:1) was ~120 kD, suggesting a dimer, whereas at high ligand:protein ratios (>~4:1) GyrA59 had a MW of ~250 kD, consistent with a tetramer. By using nanoelectrospray ionization mass spectrometry (nanoESI MS) under conditions where noncovalent interactions are preserved, we assessed the binding of SD8 to GyrA59 and full-length GyrA. In the absence of SD8, both proteins had MWs consistent with dimers (fig. S4). Titration of SD8 into solutions containing the proteins showed dimeric species with either one or two SD8 molecules bound at ligand:protein ratios of <~2:1. With a ligand:protein ratio of 3:1, we began to see formation of a tetrameric species, which increased with increasing SD8 concentrations to become the predominant species at ~7.5:1 (fig. S4). These experiments showed small amounts of three SD8 molecules bound per dimer but no evidence of four, suggesting that a tetramer readily forms once four molecules are bound (fig. S4). We suggest that the dimeric species, observed at limiting ligand concentrations, might represent a single SD8 molecule bound to the AC and PK pockets within the same subunit (fig. S3).

To probe the importance of the two binding pockets, we analyzed the interactions of GyrA59 with simocyclinone analogs lacking either the PK or the AC moiety (Fig. 1). Simocyclinone C4 is a naturally occurring intermediate in the SD8 pathway that lacks the AC moiety; MGD8N2A, which lacks the PK moiety, was generated by chemical hydrolysis of SD8. The parent compound has a minimum inhibitory concentration (IC_{50}) value of 0.6 μM for inhibition of gyrase supercoiling, whereas IC_{50} values of 70 and 50 μM were obtained for analogs lacking either the AC or the PK moiety, respectively (Fig. 1). Although inhibition is greatly reduced, the fact that these SD8 analogs have some activity suggests that cross-linking of the two GyrA dimers is not a prerequisite for inhibition.

One key issue was to establish the in vivo target of simocyclinones; recent transcriptional profiling studies (*20*) suggest but do not prove that gyrase is the target. To address this, we selected spontaneous resistant mutants in *E. coli*. Wild-type *E. coli* and other Gram-negative bacteria are resistant to simocyclinones because the compounds cannot penetrate the outer membrane (*15*); we therefore used an *E. coli* strain (NR698) that is sensitive because it carries an in-frame de-

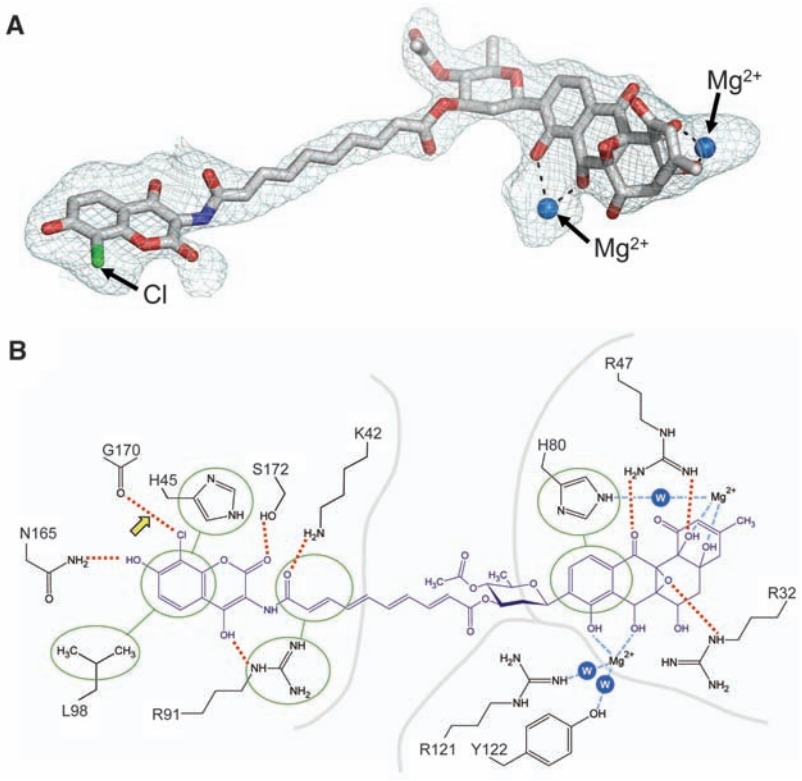

Fig. 3. Binding of SD8 to GyrA. (**A**) Simulated annealing omit electron density map for SD8 contoured at 6 σ and superposed on the final coordinates of the ligand (*27*). (**B**) Schematic figure detailing protein-ligand interactions in the GyrA59-SD8 complex. Red dotted lines represent hydrogen bonds and the single halogen bond (indicated by yellow arrow; see fig. S1). Interactions with the Mg^{2+} ions are shown as pale blue dashed lines. The side chains of Arg^{121} and Tyr^{122} (in the active site) point toward the SD8 molecule across the dimer interface and could interact with it via water molecules (blue shaded circles labeled "W") coordinated to a Mg^{2+} ion. Similarly, His^{80} likely makes a water-mediated interaction with the second Mg^{2+} ion. Nonbonded interactions are represented by the linked green ovals, which encircle the groups involved; subunit boundaries are delineated by gray lines.

Table 1. Properties of simocyclinone- and quinolone-resistant GyrA mutants. NA indicates not applicable. Mutant H78A is not active; K_D for simocyclinone is ~10 times that of wild type. S83W data is from (*19*).

GyrA mutation	Relative IC_{50} (supercoiling)	
	Simocyclinone	Ciprofloxacin
Wild type	1 (0.6 μM)*	1 (0.7 μM)*
Mutations in the simocyclinone-binding site		
Aminocoumarin-binding pocket mutations		
H45A	9.1	2.2
R91A	20	1.1
Polyketide-binding pocket mutations		
H78A	NA	NA
H80A	230	2.8
Mutations in both pockets		
H45A and H80A	>500	2.3
Mutations in the quinolone-resistance–determining region of GyrA		
G81D	40	24
S83W	10	30
A84P	38	28
D87A	7.2	5.2
D87Y	57	30
S83A and D87A	8.3	12

*Actual IC_{50} values are given in parentheses.

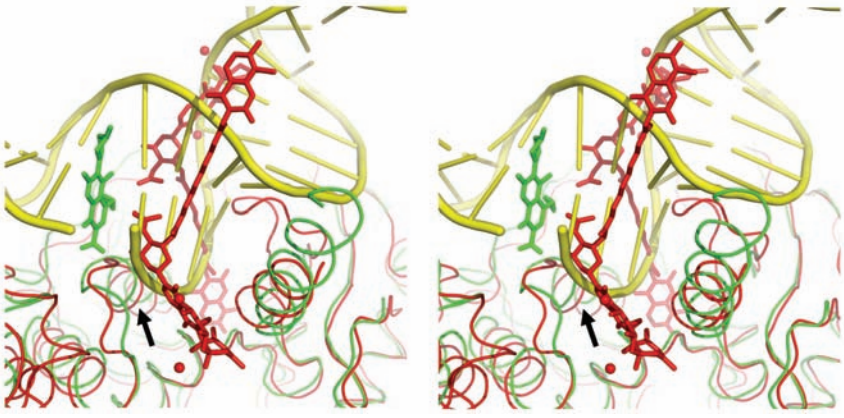

Fig. 4. Stereo view showing a superposition of GyrA59-SD8 and the clinafloxacin-DNA cleavage complex of topo IV [Protein Data Bank (PDB) code 3FOE], focusing on the drug-binding sites in one half of the GyrA/ParC dimers (*28*). The protein backbones are shown as ribbons and the drug molecules in stick representation, with GyrA59-SD8 in red, ParC-clinafloxacin in green, and the DNA from the latter structure in yellow. For clarity, the ParE subunits have been omitted from 3FOE. The SD8 and clinafloxacin binding sites are adjacent but do not overlap. This figure illustrates how SD8 would interfere with DNA binding; this would also be the case if the drug were bound in the "bent-over" conformation proposed in fig. S3. The arrow indicates the position of α-helix 4.

letion in the *imp* (increased membrane permeability) gene (*22*). We isolated 31 spontaneous simocyclinone-resistant mutants and in each case sequenced a ~500–base pair (bp) region of *gyrA*, corresponding to residues Met^{26} to Ser^{172} of the protein. We found *gyrA* mutations in 22 of them, conferring one of the following amino acid changes: V^{44}→G^{44} (V44G) (*23*), H45Y, H45Q, G81S, and D87Y (fig. S5). These amino acids are close to the bound SD8 molecule in the crystal structure, consistent with gyrase being the in vivo target. Unlike the 22 *gyrA* mutants, the remaining nine isolates had also acquired resistance to bile salts, suggesting that they could be accounted for by spontaneous second-site mutations that are known to restore outer membrane impermeability to the *imp* mutant (*22*).

On the basis of the spontaneous mutations and the crystal structure information, we made selected site-directed mutations in GyrA to probe its interaction with SD8 in vitro. The mutant proteins, together with wild-type GyrB, were assayed for DNA supercoiling in the presence of SD8 (Table 1). Mutations in either the AC (His^{45} and Arg^{91}) or the PK (His^{80} and Gly^{81}) pocket showed simocyclinone-resistant supercoiling. SD8 binding to an inactive mutant in the PK pocket, H78A (*23*), was investigated by surface-plasmon resonance using the GyrA59 protein. The mutant showed decreased binding affinity for SD8 (K_D values were 1.3 μM for wild type and 10.4 μM for H78A) and had a near-identical far-ultraviolet circular dichroism spectrum to wild-type GyrA, suggesting that it was properly folded.

Quinolone-resistant mutations map to both *gyrA* and *gyrB* in regions known as the quinolone-resistance determining regions [QRDRs (*24*, *25*)]. In the case of *E. coli* GyrA, the QRDR occurs between amino acids 67 and 106 with mutations identified at Ala^{67}, Gly^{81}, Asp^{82}, Ser^{83}, Ala^{84}, Asp^{87}, and Gln^{106} (*26*), mostly occurring either in or just before α-helix 4 (*21*) (fig. S5). From the published structures of quinolone-DNA cleavage complexes of *Streptococcus pneumoniae* topo IV (*27*), we can infer the location of the quinolone-binding site in GyrA, which is adjacent to but not overlapping the SD8 binding sites (Fig. 4). The quinolones do not make substantive contacts with the topo IV ParC protein, being closest to the equivalents of residues Gly^{81} to Ala^{84} and Asp^{87} in GyrA. Therefore, at least some of the mutations in the QRDR of GyrA most likely have indirect effects on quinolone binding. Given the proximity of the quinolone and SD8 binding sites, we investigated whether there was any cross-resistance between the two types of inhibitor. SD8-resistant mutants were tested for their susceptibility to the fluoroquinolone ciprofloxacin, and a range of ciprofloxacin-resistant mutants were tested for their susceptibility to SD8 (Table 1).

Mutations in the simocyclinone-binding pockets (AC and PK) result in near–wild-type amounts of susceptibility to ciprofloxacin (Table 1); QRDR mutations in α-helix 4 of GyrA confer increased resistance to both ciprofloxacin and SD8. None of these amino acids makes direct contacts with bound SD8 (Fig. 3B); given the low resolution of the quinolone-DNA-topo IV complex structures, it is not possible to precisely define any ligand-protein interactions, but it is likely that substitutions at positions 81 to 84 and 87 in GyrA would have an effect on drug binding. The prevalence of mutations at Ser^{83} and Asp^{87} in quinolone-resistant clinical isolates supports this assertion (*26*). In the case of SD8, it is possible that mutations in α-helix 4 of GyrA, which lies between the AC and PK binding pockets, can affect the proposed bridging of the two binding sites by the tetraene linker (fig. S3).

Given the global concerns over drug-resistant bacterial diseases, work on SD8 raises the prospect of developing agents that exploit its bifunctional mode of antibiotic action on a well-validated target. Alternatively, designing monofunctional compounds with enhanced affinity for one or the other of the binding sites may prove fruitful.

References and Notes

1. A. D. Bates, A. Maxwell, *DNA Topology* (Oxford Univ. Press, Oxford, 2005).
2. A. J. Schoeffler, J. M. Berger, *Q. Rev. Biophys.* **41**, 41 (2008).
3. A. D. Bates, A. Maxwell, *Biochemistry* **46**, 7929 (2007).
4. A. Maxwell, *Trends Microbiol.* **5**, 102 (1997).
5. C. M. Oliphant, G. M. Green, *Am. Fam. Physician* **65**, 455 (2002).
6. D. Livermore, *J. Antimicrob. Chemother.* **60** (suppl. 1), i59 (2007).
7. A. Maxwell, D. M. Lawson, *Curr. Top. Med. Chem.* **3**, 283 (2003).
8. V. Lamour, L. Hoermann, J. M. Jeltsch, P. Oudet, D. Moras, *J. Biol. Chem.* **277**, 18947 (2002).
9. F. T. F. Tsai *et al.*, *Proteins* **28**, 41 (1997).
10. G. A. Holdgate *et al.*, *Biochemistry* **36**, 9663 (1997).
11. R. J. Lewis *et al.*, *EMBO J.* **15**, 1412 (1996).
12. S.-M. Li, L. Heide, *Curr. Med. Chem.* **12**, 419 (2005).
13. C. Anderle *et al.*, *Antimicrob. Agents Chemother.* **52**, 1982 (2008).
14. R. H. Flatman, A. Eustaquio, S. M. Li, L. Heide, A. Maxwell, *Antimicrob. Agents Chemother.* **50**, 1136 (2006).
15. J. Schimana *et al.*, *J. Antibiot. (Tokyo)* **53**, 779 (2000).
16. U. Theobald, J. Schimana, H. P. Fiedler, *Antonie Leeuwenhoek* **78**, 307 (2000).
17. U. Galm *et al.*, *Arch. Microbiol.* **178**, 102 (2002).
18. A. Trefzer *et al.*, *Antimicrob. Agents Chemother.* **46**, 1174 (2002).
19. R. H. Flatman, A. J. Howells, L. Heide, H.-P. Fiedler, A. Maxwell, *Antimicrob. Agents Chemother.* **49**, 1093 (2005).
20. L. M. Oppegard *et al.*, *Antimicrob. Agents Chemother.* **53**, 2110 (2009).
21. J. H. Morais Cabral *et al.*, *Nature* **388**, 903 (1997).
22. N. Ruiz, B. Falcone, D. Kahne, T. J. Silhavy, *Cell* **121**, 307 (2005).
23. Single-letter abbreviations for the amino acid residues are as follows: A, Ala; C, Cys; D, Asp; E, Glu; F, Phe; G, Gly; H, His; I, Ile; K, Lys; L, Leu; M, Met; N, Asn; P, Pro; Q, Gln; R, Arg; S, Ser; T, Thr; V, Val; W, Trp; and Y, Tyr.
24. H. Yoshida, M. Bogaki, M. Nakamura, L. M. Yamanaka, S. Nakamura, *Antimicrob. Agents Chemother.* **35**, 1647 (1991).
25. H. Yoshida, M. Bogaki, M. Nakamura, S. Nakamura, *Antimicrob. Agents Chemother.* **34**, 1271 (1990).
26. D. C. Hooper, E. Rubinstein, *Quinolone Antimicrobial Agents* (American Society for Microbiology, Washington, DC, ed. 3, 1993), p. 485.
27. Materials and methods are available as supporting material on *Science* Online.
28. I. Laponogov *et al.*, *Nat. Struct. Mol. Biol.* **16**, 667 (2009).

29. This work was funded by UK Biotechnology and Biological Sciences Research Council (BBSRC) and the European Commission (CombiGyrase LSHB-CT-2004-503466); M.J.E. was supported by a CASE studentship funded by BBSRC and Plant Bioscience Limited, and T.B.K.L. was supported by a John Innes Centre Rotation studentship. We thank A. Zeeck (University of Göttingen) for providing us with a sample of MGD8N2A; P. Johnson for assistance with CD experiments; R. Field, L. Heide, and D. Hopwood for helpful discussions; and N. Ruiz and T. Silhavy for their advice and for the *E. coli imp4213* mutant. Atomic coordinates and structure factors have been deposited in the Protein Data Bank with accession code 2WL2. We dedicate this paper to the memory of Chris Lamb, director of the John Innes Centre from 1999 to 2009.

Supporting Online Material

www.sciencemag.org/cgi/content/full/326/5958/1415/DC1
Materials and Methods
SOM Text
Figs. S1 to S5
Tables S1 and S2

15 July 2009; accepted 8 October 2009
10.1126/science.1179123